



Published in final edited form as:

Cell Rep. 2015 October 27; 13(4): 771–782. doi:10.1016/j.celrep.2015.09.044.

## Antagonizing Neuronal Toll-like Receptor 2 Prevents Synucleinopathy by Activating Autophagy

Changyoun Kim<sup>1,2</sup>, Edward Rockenstein<sup>2</sup>, Brian Spencer<sup>2</sup>, Hyung-Koo Kim<sup>1</sup>, Anthony Adame<sup>2</sup>, Margarita Trejo<sup>2</sup>, Klodjan Stafa<sup>2</sup>, He-Jin Lee<sup>3</sup>, Seung-Jae Lee<sup>1,\*</sup>, and Eliezer Masliah<sup>2,\*</sup>

<sup>1</sup>Neuroscience Research Institute, Department of Medicine, Seoul National University College of Medicine, Seoul 110-799, Korea

<sup>2</sup>Department of Neurosciences and Pathology, School of Medicine, University of California, San Diego, La Jolla, CA 92093, USA

<sup>3</sup>Department of Anatomy, School of Medicine, Konkuk University, Seoul 143-701, Korea

### SUMMARY

Impaired autophagy has been implicated in many neurodegenerative diseases, such as Parkinson's disease (PD), and might be responsible for deposition of aggregated proteins in neurons. However, little is known how neuronal autophagy and clearance of aggregated proteins are regulated. Here, we show a role for Toll-like receptor 2 (TLR2), a pathogen-recognizing receptor in innate immunity, in regulation of neuronal autophagy and clearance of  $\alpha$ -synuclein, a protein aggregated in synucleinopathies, including PD. Activation of TLR2 resulted in accumulation of  $\alpha$ -synuclein aggregates in neurons as a result of inhibition of autophagic activity through regulation of the AKT/mTOR pathway. In contrast, inactivation of TLR2 resulted in autophagy activation and increased clearance of neuronal  $\alpha$ -synuclein, hence reduced neurodegeneration, in transgenic mice and in *in vitro* models. These results uncover novel roles of TLR2 in regulating neuronal autophagy, and the TLR2 pathway may be targeted for the autophagy activation strategies in treating neurodegenerative disorders.

### Graphical Abstract

\*Correspondence: sjlee66@snu.ac.kr (S.-J.L.), emasliah@ucsd.edu (E.M.).

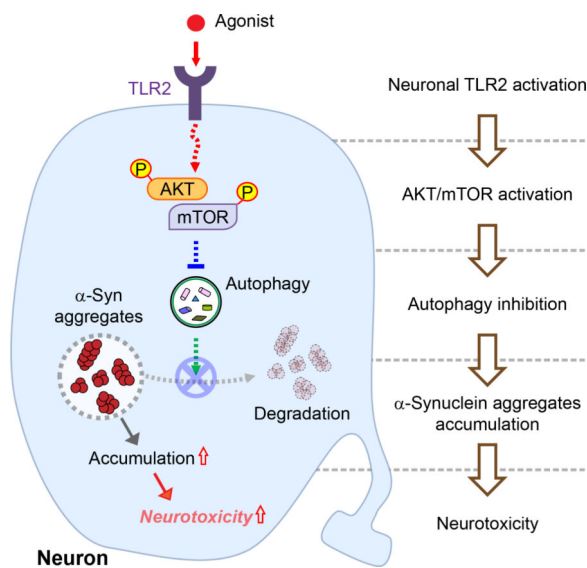
**Publisher's Disclaimer:** This is a PDF file of an unedited manuscript that has been accepted for publication. As a service to our customers we are providing this early version of the manuscript. The manuscript will undergo copyediting, typesetting, and review of the resulting proof before it is published in its final citable form. Please note that during the production process errors may be discovered which could affect the content, and all legal disclaimers that apply to the journal pertain.

#### AUTHOR CONTRIBUTIONS

C.K., S.-J.L., and E.M. conceived and designed the study, and analyzed the data. C.K. performed majority of experiments; *in vitro* cell culture experiments, biochemical analysis, quantitative polymerase chain reaction analysis, and cytotoxicity analysis. E.R. and E.M. designed and performed mice lentiviral vectors injection experiment. C.K., H.-K.K., H.-J.L., and S.-J.L. designed and generated A53T<sup>+</sup>Tr2<sup>-/-</sup> mice. C.K. and A.A. performed all immunohistochemical and immunolabeling experiment. M.T. performed electron microscopy analysis. B.S. constructed lentiviral vectors and involved in manuscript preparation. C.K. and K.S. generated and cultured neural precursor cells. C.K., S.-J.L., and E.M. wrote the manuscript.

#### SUPPLEMENTAL INFORMATION

Supplemental Information includes seven Supplemental Figures, one Supplemental table, Supplemental Experimental Procedures, and Supplemental references and can be found with this article online at



## INTRODUCTION

Protein homeostasis (proteostasis) is vital for neuronal function and survival, as most neurons are not renewable. Impaired proteostasis results in protein aggregation and has been suggested to be the crucial step in the pathogenesis of many neurodegenerative diseases. Maintaining the healthy neuronal proteostasis state is therefore one of foremost importance. However, the mechanism of how proteostasis is regulated in neurons remains largely unknown.

Abnormal deposition of  $\alpha$ -synuclein in neuron and glia is implicated in a group of neurodegenerative diseases that include Parkinson's disease (PD), dementia with Lewy bodies (DLB), and multiple system atrophy (MSA) (McCann et al., 2014). In PD, the  $\alpha$ -synuclein pathology initiates at specific brain regions and disseminates to various anatomical regions as the clinical symptoms progress (Braak and Del Tredici, 2008). Cell-to-cell transmission of  $\alpha$ -synuclein aggregates have been suggested to be involved in the pathological progression of the disease (Lee et al., 2014). The mechanisms of  $\alpha$ -synuclein aggregation and transmission are not entirely clear; however, studies suggest that alterations in synthesis and clearance processes play crucial roles (Bae et al., 2014; Kim and Lee, 2008; Lee et al., 2014).

Macroautophagy (hereafter referred to as autophagy) is a lysosome-dependent cellular degradation system that is known to be responsible for the clearance of protein aggregates in neuron (Menzies et al., 2014). Therefore, inhibition of lysosomal and autophagic functions resulted in the accumulation of  $\alpha$ -synuclein aggregates in cells (Lee et al., 2004; Webb et al., 2003). In contrast, activation of autophagy promoted clearance of the cytoplasmic protein aggregates, such as  $\alpha$ -synuclein and polyglutamine proteins (Menzies et al., 2014). These results led to the proposal that enhancement of autophagic activity might be a promising therapeutic strategy for neurodegenerative diseases (Ravikumar et al., 2004; Sarkar et al., 2007; Sarkar et al., 2005).

Despite the importance of autophagy in proteostasis, the regulation of neuronal autophagy is poorly understood. In particular, very little is known about the extracellular cues that regulate autophagy in the nervous system. However, regulation of autophagy by extracellular stimuli has been intensively studied in immune cells, because autophagy plays important roles in response to extracellular pathogens (Delgado and Deretic, 2009). Pattern recognition receptors (PRRs), including toll-like receptors (TLRs), are well known regulators of pathogen-related autophagy (Delgado and Deretic, 2009; Delgado et al., 2008).

TLR2 has been suggested to play an important role in the pathogenesis of neurodegenerative diseases through involvement in neuroinflammatory processes. TLR2 is upregulated in PD and DLB patients as well as in animal models of neurodegenerative diseases, including AD and PD/DLB (Kim et al., 2013; Letiembre et al., 2009). In this report we investigated the role of TLR2 signaling in the regulation of autophagy and  $\alpha$ -synuclein clearance in neurons. We provide evidence that TLR2 signaling is inhibitory for autophagy, hence for clearance of  $\alpha$ -synuclein aggregates, in neurons.

## RESULTS

### ***Tlr2*-deficiency Results in Reduced Neuronal $\alpha$ -synuclein Accumulation and Neurodegeneration in a Mouse Model of Synucleinopathy**

Our previous study demonstrated that oligomeric forms of neuron-released  $\alpha$ -synuclein induced the activation of microglia by interaction with TLR2 on the surface of microglia (Kim et al., 2013). To gain a comprehensive understanding for the pathological roles of TLR2 in PD, we generated A53T<sup>+</sup>*Tlr2*<sup>-/-</sup> mice by crossing transgenic mice (tg) expressing human A53T  $\alpha$ -synuclein (A53T<sup>+</sup>) and *Tlr2* knockout mice (*Tlr2*<sup>-/-</sup>) (Figures 1A and S1A). The mRNA levels of human  $\alpha$ -synuclein were not significantly affected by *Tlr2* gene deletion as determined by quantitative PCR (Figure S1B and Table S1). However, the levels of  $\alpha$ -synuclein in Triton X-100-insoluble brain homogenates were significantly decreased in A53T<sup>+</sup>*Tlr2*<sup>-/-</sup> mice compared with those in A53T<sup>+</sup> mice (Figures 1B and S1C). Immunoreactivity against  $\alpha$ -synuclein was also significantly reduced in neurons of A53T<sup>+</sup>*Tlr2*<sup>-/-</sup> mice compared to A53T<sup>+</sup> mice (Figure 1C).

To verify *Tlr2*-expressing cells in the brain, we performed immunofluorescence analysis (Figures 1D-1F). *Tlr2* was expressed in both NeuN-positive neurons and Iba-1-positive microglia in the brain (Figures 1D-1F). In contrast, *Thr2* was not detected in either microglia or neurons in A53T<sup>+</sup>*Tlr2*<sup>-/-</sup> (Figures 1D-1F) or *Tlr2*<sup>-/-</sup> mice (data not shown). Furthermore, the percentage of *Tlr2*-positive neurons was increased in A53T<sup>+</sup> mice compared to the non-tg mice (Figure 1F).

To confirm the alterations of  $\alpha$ -synuclein levels in tg mice, we performed immunohistochemical analysis (Figures 2A-2E and S2).  $\alpha$ -synuclein was highly expressed in neuronal cell bodies and the neuropil throughout the brain in A53T<sup>+</sup> mice (Figures 2A-2E and S2A). In contrast, levels of  $\alpha$ -synuclein were significantly decreased in both cell bodies (Figures 2A-2C and 2E) and the neuropil (Figures 2A and 2D) of A53T<sup>+</sup>*Tlr2*<sup>-/-</sup> mice compared to A53T<sup>+</sup> mice. To further support our findings, we used an antibody that specifically recognizes the C-terminus of human  $\alpha$ -synuclein (Figures S2D-S2H). As

expected, human  $\alpha$ -synuclein was not detected in non-tg or *Tlr2*<sup>-/-</sup> mice, but highly expressed in neuronal cell bodies and the neuropil of A53T<sup>+</sup> mice (Figures S2D-S2H). In contrast, human  $\alpha$ -synuclein immunoreactivity was clearly decreased in A53T<sup>+</sup>*Tlr2*<sup>-/-</sup> mice compared to A53T<sup>+</sup> mice (Figures S2D-S2H). Together, these results suggest that neuronal TLR2 plays a role in the regulation of steady state levels of  $\alpha$ -synuclein.

Overexpression of human  $\alpha$ -synuclein has been shown to induce neuroinflammation and neurodegeneration in mice (Hirsch and Hunot, 2009; Long-Smith et al., 2009; Maries et al., 2003). Likewise, in the neocortex of the A53T<sup>+</sup> mice, immunohistochemical analysis showed increases in astrogliosis (GFAP), microgliosis (Iba-1), and neurodegeneration (NeuN) (Figures 2F-2I). In addition, the mRNA levels of pro-inflammatory cytokine genes, such as TNF $\alpha$  and IL-6, were increased in the neocortices of A53T<sup>+</sup> mice (Figures S2B and S2C). In contrast, gene deletion of *Tlr2* significantly reduced glial activation, neuronal loss, and cytokine gene expressions in A53T<sup>+</sup>*Tlr2*<sup>-/-</sup> mice (Figures 2F-2I and S2B and S2C), suggesting that reduction of  $\alpha$ -synuclein levels in *Tlr2*-deficient mice alleviates the pathogenic phenotypes, such as neuroinflammation and neurodegeneration.

### Activation of TLR2 Leads to Accumulation of $\alpha$ -Synuclein Aggregates and $\alpha$ -synuclein-dependent Neurotoxicity in Neurons

To investigate the mechanism of TLR2-mediated  $\alpha$ -synuclein accumulation, differentiated SH-SY5Y human neuroblastoma cells (dSY5Y) were infected with either lentiviral vectors overexpressing  $\alpha$ -synuclein (LV- $\alpha$ -Syn) or control vector (LV-control), and treated with TLR2-specific agonists, pam3CSK4 (TLR1/2 agonist) (Figures 3A-3C). Expression of TLR2 in dSY5Y cells was demonstrated by quantitative PCR and the TLR2 ligand response assay (Figures S3A and S3B). Immunofluorescence analysis showed that the levels of  $\alpha$ -synuclein were increased in TLR2 agonist-exposed cells (Figure 3A). In addition, the Triton-insoluble  $\alpha$ -synuclein oligomers were increased by TLR2 activation in cells (Figure 3B). In contrast, pre-treatment with TLR2 functional blocking antibody (T2.5) significantly inhibited the agonist-induced accumulation of  $\alpha$ -synuclein oligomers in cells (Figure 3C).

To confirm the involvement of TLR2 in accumulation of  $\alpha$ -synuclein oligomers in neuronal cells, we constructed a TLR2 knockdown lentiviral vector (LV-sh.TLR2) (Figures S4A and S4B). Knockdown of TLR2 expression decreased I $\kappa$ B degradation by TLR2 agonist (Figure S4C), and significantly reduced the TLR2 agonist-induced accumulation of  $\alpha$ -synuclein oligomers in dSY5Y cells (Figure 3D). Overexpression of  $\alpha$ -synuclein showed cytotoxicity in dSY5Y cells, and activation of TLR2 exacerbated the cytotoxicity (Figures 3E and S3C). In contrast, knockdown or functional blocking of TLR2 alleviated the cytotoxicity induced not only by  $\alpha$ -synuclein overexpression alone but also by  $\alpha$ -synuclein expression with TLR2 activation (Figures 3E and S3C). These results suggest that activation of TLR2 causes accumulation of cytotoxic  $\alpha$ -synuclein oligomers in neuronal cells.

### Knockdown of TLR2 Ameliorates $\alpha$ -Synuclein Pathology and Motor Behavioral Deficits in a Mouse Model of PD

To further confirm the role of TLR2 in  $\alpha$ -synuclein pathology, we delivered the LV-sh.TLR2 into the hippocampus and the striatum of another human  $\alpha$ -synuclein tg mouse line

( $\alpha$ -Syn tg, D Line) which replicates some of the behavioral and neuropathological features similar to those observed in PD (Rockenstein et al., 2002) (Figure 4). Delivery of LV-sh.TLR2 reduced the expression of Tlr2 in the hippocampus of both non-tg and  $\alpha$ -Syn tg mice (Figures 4A, 4B, and S4D) and resulted in a significant decrease of  $\alpha$ -synuclein levels (Figures 4A, 4C, and S4D). The expressions of the striatal Tlr2 and the  $\alpha$ -synuclein accumulation were also decreased by injection of LV-sh.TLR2 (data not shown). The  $\alpha$ -Syn tg mice showed astrogliosis and microglia activation (Kim et al., 2013; Spencer et al., 2014), and delivery of LV-sh.TLR2 significantly decreased both microglia activation and astrogliosis in this model (Figures 4A, 4D, and 4E). Similar to our previous results, immunohistochemical analysis showed that expression of Tlr2 was increased in the  $\alpha$ -Syn tg mice compared to non-tg mice (Kim et al., 2013) (Figures 4A, 4B, and S4D).

In order to investigate the effects of the TLR2 knockdown on motor behavior in  $\alpha$ -Syn tg mice, we performed the beam break test using non-tg and  $\alpha$ -Syn tg mice which were injected with either LV-sh.control or LV-sh.TLR2 (Figures 4F and 4G).  $\alpha$ -Syn tg showed an increment of the beam break numbers (Valera et al., 2015); however it was significantly decreased by the injection of LV-sh.TLR2 (Figure 4F). The numbers of beam breaks obtained from non-tg and  $\alpha$ -Syn tg mice were decreased by daily repetition tests, but the daily reduction rate of  $\alpha$ -Syn tg was significantly slower than the rates obtained from non-tg mice (Figure 4G). Interestingly, LV-shTLR2-injected  $\alpha$ -Syn tg mice showed similar reduction rate of daily beam break numbers with non-tg mice (Figure 4G). Taken together, these results suggest that knockdown of TLR2 ameliorates motor behavioral deficits and  $\alpha$ -synuclein pathology in a mouse model of PD.

### **Activation of Neuronal TLR2 Leads to $\alpha$ -synuclein Accumulation via Autophagy Dysregulation through AKT/mTOR Activation**

Since mRNA levels of  $\alpha$ -synuclein were not affected by *Tlr2* gene deletion (Figure S1B), we hypothesized that protein degradation systems are regulated by TLR2 activation. In particular, we examined the autophagy system, an active degradation mechanism for aggregation-prone proteins (Kiselyov et al., 2007).  $\alpha$ -synuclein-overexpressing dSY5Y cells were treated with pam3CSK4 together with either the autophagy inhibitor (Bafilomycin A1) or autophagy inducer (Rapamycin) (Figure 5A). Activation of TLR2 significantly increased the accumulation of  $\alpha$ -synuclein oligomers and p62/SQSTM1 in dSY5Y cells (Figure 5A). Inhibition of autophagy also resulted in accumulation of  $\alpha$ -synuclein oligomers and p62/SQSTM1 (Figure 5A). Co-treatment of cells with pam3CSK4 and the autophagy inhibitor did not further increase the accumulation of  $\alpha$ -synuclein from the bafilomycin A1 treatment alone (Figure 5A), suggesting that the effects of TLR2 agonist on  $\alpha$ -synuclein are exerted through the autophagy pathway. However, the co-treatment showed an additive increment of p62/SQSTM1 accumulation (Figure 5A). The reason for additive increment of p62/SQSTM1 expression probably stems from the positive-transcriptional feedback by autophagy (Sahani et al., 2014). Consistent with these results, induction of autophagy alleviated the effect of TLR2 agonist on accumulation of  $\alpha$ -synuclein oligomers and p62/SQSTM1 in dSY5Y cells (Figure 5A).

To visualize live autophagy flux, dSY5Y cells were infected with either LV-LC3-GFP or LV-LC3-GFP-mCherry (pH-sensitive-GFP-mCherry tag) (Figures 5C, 5D, and S5A). Treatment of rapamycin increased the number of LC3-GFP puncta (Figures 5C and S5A) and LC3-mCherry puncta (Figure 5D) in dSY5Y cells; however, activation of TLR2 decreased the number of LC3-GFP and LC3-mCherry puncta while increasing  $\alpha$ -synuclein immunoreactivity (Figures 5C, 5D, and S5A). In addition, co-treatment of rapamycin with pam3CSK4 significantly decreased the accumulation of  $\alpha$ -synuclein caused by pam3CSK4 in the cells and increased formation of LC3-GFP and LC3-mCherry puncta, suggesting that rapamycin, a mammalian target of rapamycin (mTOR) inhibitor, could suppress TLR2-mediated autophagy inhibition (Figures 5C and 5D). Taken together, these results suggest that activation of TLR2 results in accumulation of  $\alpha$ -synuclein via autophagy inhibition, which can be reversed by rapamycin-mediated autophagy induction.

To verify the regulation of autophagy by TLR2, we constructed and infected dSY5Y cells with either LV-ATG7 or LV-sh.ATG7 (Figure 5B). Interestingly, overexpression of ATG7 significantly decreased accumulation of  $\alpha$ -synuclein oligomers by pam3CSK4 as well as the basal levels of  $\alpha$ -synuclein oligomers in the cells (Figure 5B). In contrast, knockdown of ATG7 increased the basal levels of  $\alpha$ -synuclein oligomers, but did not further increase the accumulation of  $\alpha$ -synuclein oligomers from the individual treatments, suggesting that the effects of the TLR2 agonist are exerted through the autophagy pathway (Figure 5B).

We next infected neuronal cells with the LV-sh.TLR2 to confirm the regulation of autophagy by TLR2 (Figure 5E). As shown earlier (Figure 3D), TLR2 agonist-driven accumulation of  $\alpha$ -synuclein oligomer and p62/SQSTM1 were completely inhibited by knockdown of TLR2 in dSY5Y cells (Figure 5E). Moreover, accumulation p62/SQSTM1 occurred 6-hours prior to the accumulation of  $\alpha$ -synuclein oligomers in pam3CSK4-exposed cells (Figure S5B). Activation of TLR2 also increased accumulation of polyubiquitinated proteins, well-known p62/SQSTM1 substrates (Figure S5C). The pam3CSK4-driven accumulation of polyubiquitinated-proteins was reduced by knockdown of TLR2, which also resulted in increased levels of LAMP2A, indicating that the lysosomal contents might be increased as a compensatory response against autophagy failure (Figure S5C).

Next, we investigated the alteration of mTOR, because autophagy inhibition by the TLR2 activation was recovered by rapamycin (Figures 5F and 5G). Surprisingly, the phosphorylation of mTOR (S2481) was increased by activation of TLR2 in dSY5Y cells (Figure 5F). In addition, activation of TLR2 also increased phosphorylation of AKT (S473), a well-known mTOR activator (Janku et al., 2011) (Figure 5F). In contrast, knockdown of TLR2 inhibited the pam3CSK4-driven phosphorylation of both AKT and mTOR, indicating that TLR2 mediates AKT/mTOR signaling pathway consistent with previous studies (Schmitz et al., 2008) (Figure 5G). Furthermore, activation of TLR2 reduced the levels of lysosomal  $\alpha$ -synuclein in  $\alpha$ -synuclein-expressing cells (V1S cells) (Figure S5D), the result consistent with the interpretation that activation of TLR2 interferes with the autophagosome formation through the AKT/mTOR activation.

We next verified our findings in human neural precursor cells (hNPCs) (Figure 6). hNPC expressed slightly higher level of TLR2 mRNA than dSY5Y cells (Figure 6A and Table S1).

The TLR2 mRNA level was significantly decreased by infection of LV-sh.TLR2 in hNPCs (Figure 6B). Activation of TLR2 induced accumulation of  $\alpha$ -synuclein oligomers and p62/SQSTM1 in hNPCs (Figure 6C). Knockdown of TLR2 inhibited the agonist-driven accumulation of both  $\alpha$ -synuclein and p62/SQSTM1 (Figure 6D). More interestingly, activation of TLR2 increased phosphorylated-AKT (S473) while the basal levels of phosphorylated-AKT were significantly decreased by TLR2 knockdown, which may be related to reduced expression of  $\alpha$ -synuclein in LV-sh.TLR2-infected hNPCs (Figure 6D). Activation of TLR2 also increased  $\alpha$ -synuclein-immunoreactivity and reduced LC3-GFP puncta in hNPCs (Figure 6E). Cytotoxicity analysis showed that overexpression of  $\alpha$ -synuclein induced neuronal cytotoxicity, which was further increased by activation of TLR2 (Figures 6F and 6G). Knockdown of TLR2 protected neurons from  $\alpha$ -synuclein-induced cytotoxicity (Figure 6F and 6G). These results suggest that activation of TLR2 results in accumulation of  $\alpha$ -synuclein oligomers and neuronal toxicity through AKT/mTOR-mediated autophagy inhibition in human neurons.

### **TLR2 Gene Depletion Promotes $\alpha$ -synuclein Clearance by Removing Autophagy Inhibition *in vivo***

To validate our findings *in vivo*, we investigated alterations of autophagy markers in mouse models (Figure S6). Double labeling analysis showed a reduction of  $\alpha$ -synuclein levels in A53T<sup>+</sup>*Tlr2*<sup>-/-</sup> mice, compared to A53T<sup>+</sup> mice (Figure S6A). In contrast, immunoreactivity against LC3 was increased in both *Tlr2*<sup>-/-</sup> and A53T<sup>+</sup>*Tlr2*<sup>-/-</sup> mice, and the latter animals showed higher levels of LC3 than the former (Figure S6A). A53T<sup>+</sup> mice showed higher levels of p62/SQSTM1 than the non-tg mice (Figure S6C), and deletion of *Tlr2* completely reversed the  $\alpha$ -synuclein-induced p62/SQSTM1 accumulation (Figure S6C). Expression levels of Beclin-1 and Lamp2a were not altered in A53T<sup>+</sup> and A53T<sup>+</sup>*Tlr2*<sup>-/-</sup> mice (Figures S6B and S6C). However, LC3I/LC3II conversion and Atg12-Atg5 conjugation were increased in A53T<sup>+</sup>*Tlr2*<sup>-/-</sup> mice (Figure S6B). The number of autophagosomes was significantly increased in both *Tlr2*<sup>-/-</sup> and A53T<sup>+</sup>*Tlr2*<sup>-/-</sup> mice (Figure S6D and S6F). Furthermore, synaptic degeneration observed by electron microscopy in A53T<sup>+</sup> mice was significantly reduced by *Tlr2* gene depletion (Figure S6D and S6E). These findings are consistent with the interpretation that TLR2 depletion, and perhaps inactivation, restores autophagy process, thereby preventing accumulation of  $\alpha$ -synuclein and neurodegeneration.

### **Inhibition of AKT Activity Results in Decrease of $\alpha$ -synuclein Accumulation by Neuronal TLR2 Activation**

To validate the roles of AKT signaling in the regulation of neuronal autophagy by TLR2, dSY5Y cells were treated with GSK690693, an AKT inhibitor.  $\alpha$ -synuclein-overexpressing dSY5Y cells were treated with pam3CSK4 together with two different concentrations of GSK690693 (Figure 7A). As shown earlier (Figures 3, 5, 6, and S5B), activation of TLR2 increased accumulation of  $\alpha$ -synuclein oligomers in neuronal cells (Figure 7A). Surprisingly, treatment of GSK690693 significantly decreased the accumulation of  $\alpha$ -synuclein and p62/SQSTM1 caused by pam3CSK4 in the cells (Figure 7A), suggesting that GSK690693, an AKT inhibitor, could suppress TLR2-mediated autophagy inhibition. Taken together, these results suggest that activation of TLR2 results in accumulation of  $\alpha$ -synuclein via AKT/mTOR-mediated autophagy inhibition in neurons.

## DISCUSSION

In the present study, we show how neuronal  $\alpha$ -synuclein pathology is regulated by extracellular signals. Activation of TLR2 resulted in  $\alpha$ -synuclein accumulation through an AKT/mTOR-dependent inhibition of autophagy. In contrast, genetic and pharmacological inactivation of the TLR2 and TLR2 downstream signaling resulted in autophagy activation, causing a dramatic decrease of  $\alpha$ -synuclein aggregation in neurons (Figure 7B). This work provides a significant advancement in our understanding of how neuronal autophagy and clearance of neuronal protein aggregates are regulated by extracellular signals.

Although much attention has been paid to the intracellular processes of  $\alpha$ -synuclein synthesis and degradation, not much is known about the extracellular cues that regulate the intracellular levels of the protein (Kim and Lee, 2008). Recent studies showed the alteration of  $\alpha$ -synuclein expression by extracellular cues, including growth factors and small molecules (Clough and Stefanis, 2007; Leng and Chuang, 2006; Mash et al., 2003). Nerve growth factor and basic fibroblast growth factor increased expression of  $\alpha$ -synuclein through the mitogen-activated protein kinase pathway (Clough and Stefanis, 2007). Expression of  $\alpha$ -synuclein is also regulated by bioactive small molecules, including valproic acid and cocaine (Leng and Chuang, 2006; Mash et al., 2003). However, here we showed how extracellular cues alter the level of  $\alpha$ -synuclein through regulation of intracellular process via gene expression. In particular, we demonstrated that TLR2, a cell surface receptor, regulates the level of  $\alpha$ -synuclein through intracellular autophagy processes in neurons.

The roles of TLRs and TLR downstream signaling cascades have been extensively investigated in microglia and astrocytes through their role in neuroinflammation; however, little is known of TLRs functions in neurons. Regardless, neuronal expressions of TLRs have been demonstrated by multiple studies (Liu et al., 2014). Expressions of TLR1, TLR2, TLR3, and TLR4 have been detected in human NT2-N neuronal cell line (Lafon et al., 2006). A TLR4 agonist, lipopolysaccharide (LPS), induced expression of TNF $\alpha$ , IL-6, CCL5, and CXCL1 in mouse cortical neurons (Leow-Dyke et al., 2012). In addition, TLR7 activation increased expression of TNF $\alpha$  and IL-6 in murine primary neurons (Liu et al., 2013). Neurons also express the TLR downstream signaling proteins, such as Myd88 and Trif (Chen et al., 2011). Furthermore, pathological and physiological functions of neuronal TLR have been discussed (Okun et al., 2011). Recent study showed that expression and activation of neuronal TLR2 and 4 contributed to neurodegeneration by ischemic stroke (Tang et al., 2007). Studies have also suggested the roles of TLRs, such as TLR3, TLR7, and TLR8, in neural morphogenesis (Liu et al., 2014). Activation of TLR3 induces growth-cone collapse and inhibits neurite outgrowth in cultured dorsal root ganglion, cortical, and hippocampal neurons (Cameron et al., 2007). Activation of TLR7 and TLR8 also negatively regulates neurite outgrowth in mouse cortical neurons (Liu et al., 2013; Ma et al., 2006). However, the mechanism as to how TLRs regulate neurite outgrowth is not understood, nor are the roles of TLRs in other neuronal functions. In this study, we also show that neurons and SH-SY5Y human neuroblastoma cells express TLR2 and react in response to TLR2-specific agonists.



The mechanism underlying the TLR-mediated autophagy regulation is largely unknown; however, a recent study demonstrated that activation of TLRs induced activation of mTOR via phosphoinositide 3 kinase/AKT pathway in bone marrow-derived macrophages and myeloid DC (Schmitz et al., 2008). In addition, rapamycin and Myd88/Trif double knockout inhibited pam3CSK4-driven phosphorylation of mTOR in the same cells (Schmitz et al., 2008). Although this study did not link the mTOR activation to autophagy regulation, plenty of other studies already demonstrated the suppression of autophagy by mTOR activation (Janku et al., 2011). In the present study, we also showed activation of AKT and mTOR by TLR2 activation in neurons, and knockdown of TLR2 expression intervened the activation of AKT and therefore, activated autophagy. These results suggest that neurons also utilize AKT/mTOR pathway in TLR2-induced regulation of autophagy.

Although activation of TLRs induced mTOR activation and thus autophagy inhibition, some studies showed an activation of autophagy by TLR signaling in immune cells. We still do not know what determines the dichotomy between the activation and inhibition of autophagy by activation of TLR signaling pathway in immune cells. However, herein, we clearly showed direct autophagy regulation by neuronal TLR2 resulting in  $\alpha$ -synucleinopathy. This evidence suggests the existence of specialized TLR2/autophagy regulatory mechanism which might be determined by cell type specificity. Perhaps, one can speculate that in the presence of pathogens, TLR2 activation in microglia activates autophagy to clear the pathogens, while TLR2 activation in neurons inhibits autophagy to reduce metabolic rates in an effort to survive in difficult times.

The results of our study have significant implications in therapy for PD and related synucleinopathies. We showed that TLR2 deficiency and inhibition could activate autophagy and decrease the levels of  $\alpha$ -synuclein oligomers in neurons. These results suggest therapeutic potential for antagonizing the TLR2 pathway in reducing synucleinopathy lesions. Previously, we have shown that in microglia, TLR2 is activated by  $\alpha$ -synuclein oligomers secreted from neurons and induces proinflammatory responses (Kim et al., 2013). This study demonstrated that blocking TLR2 signaling could alleviate  $\alpha$ -synuclein-induced inflammation in mice. In addition, these findings allow speculation that the neuron-released  $\alpha$ -synuclein oligomers may activate neuronal TLR2 which results in autophagy disruption and  $\alpha$ -synuclein deposition. Therefore, antagonizing the TLR2 pathway might have therapeutic benefits through both neuron-based and microglia-based mechanisms. In neurons, inhibition of TLR2 induces autophagy and decreases the levels of oligomeric  $\alpha$ -synuclein, hence reducing the  $\alpha$ -synuclein burden, while in microglia, TLR2 inhibition reduces proinflammatory responses triggered by neuron-secreted  $\alpha$ -synuclein oligomers (Figure S7). Taken together, we suggest that TLR2 and the downstream signaling may be therapeutic targets that can act on both neurons and glia, alleviating both synucleinopathy lesions and neuroinflammation.

## EXPERIMENTAL PROCEDURES

### Animals, Generation of Double Transgenic Mice, and Delivery of Lentiviral Vectors

C57Bl/6 and A53T [B6.Cg-tg(Thy1-SCNA\*A53T)1Sud/J] mice were purchased from the Jackson Laboratory (Bar Harbor, ME) (Lee et al., 2011). *Tlr2*-knockout mice were obtained

from Oriental Bioservice, Inc. (Kyoto, Japan) (Takeuchi et al., 1999). Transgenic mice expressing wild type human  $\alpha$ -synuclein under the PDGF- $\beta$  promoter ( $\alpha$ -Syn tg, D line) were described elsewhere (Masliah et al., 2000). A53T<sup>+</sup>*Tlr2*<sup>-/-</sup> mice were generated as depicted in Figure 1a. A53T<sup>+</sup>*Tlr2*<sup>-/-</sup> mice, were generated in a two-step process: step I, A53T<sup>+</sup> mice were bred with *Tlr2*<sup>-/-</sup> mice to generate A53T<sup>+</sup>*Tlr2*<sup>+/-</sup> mice, and step II, A53T<sup>+</sup>*Tlr2*<sup>+/-</sup> mice were also crossed with A53T<sup>+</sup>*Tlr2*<sup>+/-</sup> mice to generate A53T<sup>+</sup>*Tlr2*<sup>-/-</sup> mice. Mice positive for human  $\alpha$ -synuclein (A53T) and negative for *Tlr2* were determined by PCR genotyping and western blot analysis (Figure S1). Two different aged mice groups (5 month and 9 month) were used for this study. To determine the roles of Tlr2 in a model of PD, we delivered either LV-sh.control or LV-sh.TLR2 into non-tg and  $\alpha$ -Syn tg mice brains as previously described (Spencer et al., 2014). Two microliters of either LV-sh.control or LV-sh.TLR2 ( $1.9 \times 10^8$  infection units) was unilaterally stereotaxically injected into hippocampus (AP; -2.0 mm, ML; 1.5 mm, and DV; -1.3 mm) and striatum (AP; 1.0 mm, ML; 1.5 mm, and DV; -3.0 mm) of the right hemisphere. Five-weeks post injection; brains were processed for immunohistochemistry analysis. All procedures for animal use were approved by Konkuk University's Animal Care and Use Committee (non-tg, *Tlr2*<sup>-/-</sup>, A53T<sup>+</sup> and A53T<sup>+</sup>*Tlr2*<sup>-/-</sup> mice) under protocol #KU11023-1 and the Institutional Animal Care and Use Committee at University of California at San Diego (non-tg and  $\alpha$ -Syn tg mice) under protocol #S02221.

### Immunofluorescence, Immunohistological, and Neuropathological Analysis

The procedure for immunofluorescence analysis for cells and brain sections have been described elsewhere (Lee and Lee, 2002; Spencer et al., 2014; Valera et al., 2015). Briefly, SH-SY5Y cells and NPCs were seeded onto poly-L-lysine coated cover slips or matrigel coated coverslips respectively. After differentiation, infection, and treatment, cells were fixed with 4% paraformaldehyde. Coverslips were incubated with primary antibodies and fluorescence-labeled secondary antibodies in sequence. Blind-coded vibratome brain sections were incubated with primary antibodies at 4°C, followed by FITC or biotinylated secondary antibodies, avidin D-HRP (ABC elite, Vector Laboratories, Burlingame, CA) and detection with the Tyramide Signal Amplification Direct system (PerkinElmer, Waltham, MA).

Immunohistological and neuropathological analysis have been described elsewhere (Valera et al., 2015). To determine  $\alpha$ -synuclein accumulation, neurodegeneration, microgliosis, and astrogliosis, we stained brain sections with human  $\alpha$ -synuclein, NeuN, Iba-1, and GFAP antibodies, respectively. Sections were imaged by Olympus BX41 microscope. The immunoreactivity levels against human  $\alpha$ -synuclein and GFAP were determined by optical density analysis using Image Quant 1.43 program (NIH) and corrected against background signal levels. The cell numbers of NeuN- and Iba-1-positive cells were determined per field ( $230 \mu\text{m} \times 184 \mu\text{m}$ ) of each animals based on cell body recognition using Image Quant 1.43 program (NIH).

### Double Immunofluorescence Labeling Analysis

The procedure for double immunofluorescence labeling analysis has been described elsewhere (Lee and Lee, 2002). Briefly, blind-coded vibratome sections were

immunolabeled with indicated primary antibodies to determine the co-localization between Tlr2 and Iba-1, Tlr2 and NeuN,  $\alpha$ -synuclein and LC3, and  $\alpha$ -synuclein and TLR2. Immunoreactivities were detected with the Tyramide Signal Amplification Direct system (PerkinElmer) or FITC tagged secondary antibodies. Sections were imaged with a Zeiss 63X (N.A. 1.4) objective on an Axiovert 35 microscope (Zeiss, Cambridge, MA) with an attached MRC 1023 LSCm system (Bio-Rad).

Antibodies and chemicals, cell culture and infection of lentiviral vectors, quantitative polymerase chain reaction, preparation of cell and tissue extracts, and western blot analysis, electron microscopy analysis, and cytotoxicity analysis are provided in the Supplemental Experimental Procedures.

### Statistical Analysis

InStat (GraphPad Software, San Diego, CA) was used for all statistical analysis. All data were analyzed for statistical significance by using unpaired *t*-tests or one-way analysis of variance (ANOVA). All data are represented as means  $\pm$  SEM.

### Supplementary Material

Refer to Web version on PubMed Central for supplementary material.

### ACKNOWLEDGEMENTS

This work was supported by NIH grants (AG18440, AG043384, and NS057096, to E.M.), National Research Foundation grants funded by the Korean Government (2013R1A6A3A03023385, to C.K. and 2010-0015188, to S.-J.L.), and the Korea Health Technology R&D Project, Ministry of Health & Welfare, Republic of Korea (HI14C00930200, to S.-J.L.).

### REFERENCES

- Bae EJ, Yang NY, Song M, Lee CS, Lee JS, Jung BC, Lee HJ, Kim S, Masliah E, Sardi SP, et al. Glucocerebrosidase depletion enhances cell-to-cell transmission of alpha-synuclein. *Nature communications*. 2014; 5:4755.
- Braak H, Del Tredici K. Invited Article: Nervous system pathology in sporadic Parkinson disease. *Neurology*. 2008; 70:1916–1925. [PubMed: 18474848]
- Cameron JS, Alexopoulou L, Sloane JA, DiBernardo AB, Ma Y, Kosaras B, Flavell R, Strittmatter SM, Volpe J, Sidman R, et al. Toll-like receptor 3 is a potent negative regulator of axonal growth in mammals. *The Journal of neuroscience : the official journal of the Society for Neuroscience*. 2007; 27:13033–13041. [PubMed: 18032677]
- Chen CY, Lin CW, Chang CY, Jiang ST, Hsueh YP. Sarm1, a negative regulator of innate immunity, interacts with syndecan-2 and regulates neuronal morphology. *The Journal of cell biology*. 2011; 193:769–784. [PubMed: 21555464]
- Clough RL, Stefanis L. A novel pathway for transcriptional regulation of alpha-synuclein. *FASEB journal : official publication of the Federation of American Societies for Experimental Biology*. 2007; 21:596–607. [PubMed: 17167067]
- Delgado MA, Deretic V. Toll-like receptors in control of immunological autophagy. *Cell death and differentiation*. 2009; 16:976–983. [PubMed: 19444282]
- Delgado MA, Elmaoued RA, Davis AS, Kyei G, Deretic V. Toll-like receptors control autophagy. *The EMBO journal*. 2008; 27:1110–1121. [PubMed: 18337753]
- Hirsch EC, Hunot S. Neuroinflammation in Parkinson's disease: a target for neuroprotection? *Lancet neurology*. 2009; 8:382–397. [PubMed: 19296921]

- Janku F, McConkey DJ, Hong DS, Kurzrock R. Autophagy as a target for anticancer therapy. *Nature reviews Clinical oncology*. 2011; 8:528–539.
- Kim C, Ho DH, Suk JE, You S, Michael S, Kang J, Joong Lee S, Masliah E, Hwang D, Lee HJ, et al. Neuron-released oligomeric alpha-synuclein is an endogenous agonist of TLR2 for paracrine activation of microglia. *Nature communications*. 2013; 4:1562.
- Kim C, Lee SJ. Controlling the mass action of alpha-synuclein in Parkinson's disease. *Journal of neurochemistry*. 2008; 107:303–316. [PubMed: 18691382]
- Kiselyov K, Jennigs JJ Jr, Rbaibi Y, Chu CT. Autophagy, mitochondria and cell death in lysosomal storage diseases. *Autophagy*. 2007; 3:259–262. [PubMed: 17329960]
- Lafon M, Megret F, Lafage M, Prehaud C. The innate immune facet of brain: human neurons express TLR-3 and sense viral dsRNA. *Journal of molecular neuroscience : MN*. 2006; 29:185–194. [PubMed: 17085778]
- Lee HJ, Bae EJ, Lee SJ. Extracellular alpha--synuclein-a novel and crucial factor in Lewy body diseases. *Nature reviews Neurology*. 2014; 10:92–98. [PubMed: 24468877]
- Lee HJ, Khoshaghideh F, Patel S, Lee SJ. Clearance of alpha-synuclein oligomeric intermediates via the lysosomal degradation pathway. *The Journal of neuroscience : the official journal of the Society for Neuroscience*. 2004; 24:1888–1896. [PubMed: 14985429]
- Lee HJ, Lee SJ. Characterization of cytoplasmic alpha-synuclein aggregates. Fibril formation is tightly linked to the inclusion-forming process in cells. *The Journal of biological chemistry*. 2002; 277:48976–48983. [PubMed: 12351642]
- Lee HJ, Suk JE, Lee KW, Park SH, Blumbergs PC, Gai WP, Lee SJ. Transmission of Synucleinopathies in the Enteric Nervous System of A53T Alpha-Synuclein Transgenic Mice. *Experimental neurobiology*. 2011; 20:181–188. [PubMed: 22355263]
- Leng Y, Chuang DM. Endogenous alpha-synuclein is induced by valproic acid through histone deacetylase inhibition and participates in neuroprotection against glutamate-induced excitotoxicity. *The Journal of neuroscience : the official journal of the Society for Neuroscience*. 2006; 26:7502–7512. [PubMed: 16837598]
- Leow-Dyke S, Allen C, Denes A, Nilsson O, Maysami S, Bowie AG, Rothwell NJ, Pinteaux E. Neuronal Toll-like receptor 4 signaling induces brain endothelial activation and neutrophil transmigration in vitro. *Journal of neuroinflammation*. 2012; 9:230. [PubMed: 23034047]
- Letiembre M, Liu Y, Walter S, Hao W, Pfander T, Wrede A, Schulz-Schaeffer W, Fassbender K. Screening of innate immune receptors in neurodegenerative diseases: a similar pattern. *Neurobiology of aging*. 2009; 30:759–768. [PubMed: 17905482]
- Liu HY, Chen CY, Hsueh YP. Innate immune responses regulate morphogenesis and degeneration: roles of Toll-like receptors and Sarm1 in neurons. *Neuroscience bulletin*. 2014; 30:645–654. [PubMed: 24993772]
- Liu HY, Hong YF, Huang CM, Chen CY, Huang TN, Hsueh YP. TLR7 negatively regulates dendrite outgrowth through the Myd88-c-Fos-IL-6 pathway. *The Journal of neuroscience : the official journal of the Society for Neuroscience*. 2013; 33:11479–11493. [PubMed: 23843519]
- Long-Smith CM, Sullivan AM, Nolan YM. The influence of microglia on the pathogenesis of Parkinson's disease. *Progress in neurobiology*. 2009; 89:277–287. [PubMed: 19686799]
- Ma Y, Li J, Chiu I, Wang Y, Sloane JA, Lu J, Kosaras B, Sidman RL, Volpe JJ, Vartanian T. Toll-like receptor 8 functions as a negative regulator of neurite outgrowth and inducer of neuronal apoptosis. *The Journal of cell biology*. 2006; 175:209–215. [PubMed: 17060494]
- Maries E, Dass B, Collier TJ, Kordower JH, Steece-Collier K. The role of alpha-synuclein in Parkinson's disease: insights from animal models. *Nature reviews Neuroscience*. 2003; 4:727–738. [PubMed: 12951565]
- Mash DC, Ouyang Q, Pablo J, Basile M, Izenwasser S, Lieberman A, Perrin RJ. Cocaine abusers have an overexpression of alpha-synuclein in dopamine neurons. *The Journal of neuroscience : the official journal of the Society for Neuroscience*. 2003; 23:2564–2571. [PubMed: 12684441]
- Masliah E, Rockenstein E, Veinbergs I, Mallory M, Hashimoto M, Takeda A, Sagara Y, Sisk A, Mucke L. Dopaminergic loss and inclusion body formation in alpha-synuclein mice: implications for neurodegenerative disorders. *Science*. 2000; 287:1265–1269. [PubMed: 10678833]

- McCann H, Stevens CH, Cartwright H, Halliday GM. alpha-Synucleinopathy phenotypes. *Parkinsonism & related disorders*. 2014; 20(Suppl 1):S62–67. [PubMed: 24262191]
- Menzies FM, Garcia-Arencibia M, Imarisio S, O'Sullivan NC, Ricketts T, Kent BA, Rao MV, Lam W, Green-Thompson ZW, Nixon RA, et al. Calpain inhibition mediates autophagy-dependent protection against polyglutamine toxicity. *Cell death and differentiation*. 2014
- Okun E, Griffioen KJ, Mattson MP. Toll-like receptor signaling in neural plasticity and disease. *Trends in neurosciences*. 2011; 34:269–281. [PubMed: 21419501]
- Ravikumar B, Vacher C, Berger Z, Davies JE, Luo S, Oroz LG, Scaravilli F, Easton DF, Duden R, O'Kane CJ, et al. Inhibition of mTOR induces autophagy and reduces toxicity of polyglutamine expansions in fly and mouse models of Huntington disease. *Nature genetics*. 2004; 36:585–595. [PubMed: 15146184]
- Rockenstein E, Mallory M, Hashimoto M, Song D, Shults CW, Lang I, Masliah E. Differential neuropathological alterations in transgenic mice expressing alpha-synuclein from the platelet-derived growth factor and Thy-1 promoters. *Journal of neuroscience research*. 2002; 68:568–578. [PubMed: 12111846]
- Sahani MH, Itakura E, Mizushima N. Expression of the autophagy substrate SQSTM1/p62 is restored during prolonged starvation depending on transcriptional upregulation and autophagy-derived amino acids. *Autophagy*. 2014; 10:431–441. [PubMed: 24394643]
- Sarkar S, Davies JE, Huang Z, Tunnacliffe A, Rubinsztein DC. Trehalose, a novel mTOR-independent autophagy enhancer, accelerates the clearance of mutant huntingtin and alpha-synuclein. *The Journal of biological chemistry*. 2007; 282:5641–5652. [PubMed: 17182613]
- Sarkar S, Floto RA, Berger Z, Imarisio S, Cordenier A, Pasco M, Cook LJ, Rubinsztein DC. Lithium induces autophagy by inhibiting inositol monophosphatase. *The Journal of cell biology*. 2005; 170:1101–1111. [PubMed: 16186256]
- Schmitz F, Heit A, Dreher S, Eisenacher K, Mages J, Haas T, Krug A, Janssen KP, Kirschning CJ, Wagner H. Mammalian target of rapamycin (mTOR) orchestrates the defense program of innate immune cells. *European journal of immunology*. 2008; 38:2981–2992. [PubMed: 18924132]
- Spencer B, Emadi S, Desplats P, Eleuteri S, Michael S, Kosberg K, Shen J, Rockenstein E, Patrick C, Adame A, et al. ESCRT-mediated Uptake and Degradation of Brain-targeted alpha-synuclein Single Chain Antibody Attenuates Neuronal Degeneration In Vivo. *Molecular therapy : the journal of the American Society of Gene Therapy*. 2014; 22:1753–1767. [PubMed: 25008355]
- Takeuchi O, Hoshino K, Kawai T, Sanjo H, Takada H, Ogawa T, Takeda K, Akira S. Differential roles of TLR2 and TLR4 in recognition of gram-negative and gram-positive bacterial cell wall components. *Immunity*. 1999; 11:443–451. [PubMed: 10549626]
- Tang SC, Arumugam TV, Xu X, Cheng A, Mughal MR, Jo DG, Lathia JD, Siler DA, Chigurupati S, Ouyang X, et al. Pivotal role for neuronal Toll-like receptors in ischemic brain injury and functional deficits. *Proceedings of the National Academy of Sciences of the United States of America*. 2007; 104:13798–13803. [PubMed: 17693552]
- Valera E, Mante M, Anderson S, Rockenstein E, Masliah E. Lenalidomide reduces microglial activation and behavioral deficits in a transgenic model of Parkinson's disease. *Journal of neuroinflammation*. 2015; 12:93. [PubMed: 25966683]
- Webb JL, Ravikumar B, Atkins J, Skepper JN, Rubinsztein DC. Alpha-Synuclein is degraded by both autophagy and the proteasome. *The Journal of biological chemistry*. 2003; 278:25009–25013. [PubMed: 12719433]

**Highlights**

- Activation of toll-like receptor 2 antagonizes autophagy in neurons.
- TLR2 regulates neuronal autophagy via the AKT/mTOR pathway.
- Inhibition of the TLR2 pathway reduces neuronal  $\alpha$ -synuclein aggregation.
- Inhibition of TLR2 rescues Lewy body disease models from neurodegeneration.

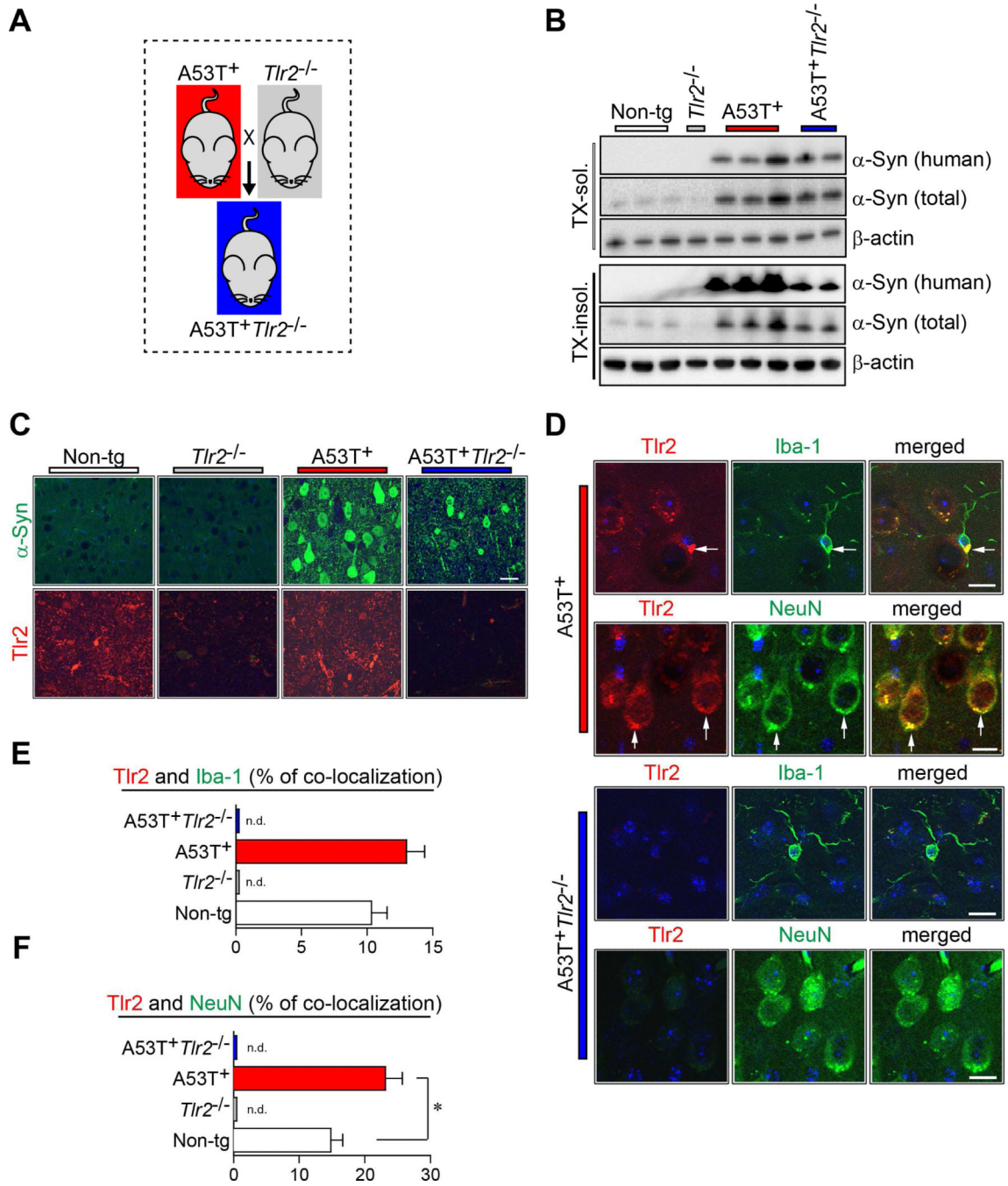


**Figure 1. Generation and Characterization of A53T<sup>+</sup> Tlr2<sup>-/-</sup> Mice**

(A) Scheme of A53T<sup>+</sup>Tlr2<sup>-/-</sup> double-tg mice generation. See Figure S1A for genotype analysis.

(B) Immunoblot analysis of Tx-soluble and Tx-insoluble brain homogenates from non-tg and tg mice (9-month) for  $\alpha$ -synuclein. See Figure S1B and S1C for  $\alpha$ -synuclein expression in the mice.

(C) Representative immunofluorescence images of non-tg and tg mice brains against human  $\alpha$ -synuclein (top panels) and Tlr2 (bottom panels) (Neocortex, 9-month-old). Sections were stained for  $\alpha$ -synuclein (green), TLR2 (red) and nuclei (DAPI, blue). Scale bar, 50  $\mu$ m.

(D) Representative images of double immunolabeling analysis for Tlr2 with either microglial marker (Iba-1) or neuronal cell marker (NeuN) in tg mice brains. Both microglial cells (top panels) and neuronal cells (bottom panels) showed immune-reactivity against Tlr2 antibody in A53T<sup>+</sup> mice brain, but not in A53T<sup>+</sup>Tlr2<sup>-/-</sup> mice brains (Neocortex, 9-month old). Scale bar, 25  $\mu$ m.

(E and F) Co-localization image analysis of Tlr2/Iba-1 (E) and Tlr2/NeuN (F) in non-tg and tg mice brains (n = 6 per each group; unpaired *t*-test; \**p* < 0.05; n.d., not detected). Data are represented as mean  $\pm$  SEM.



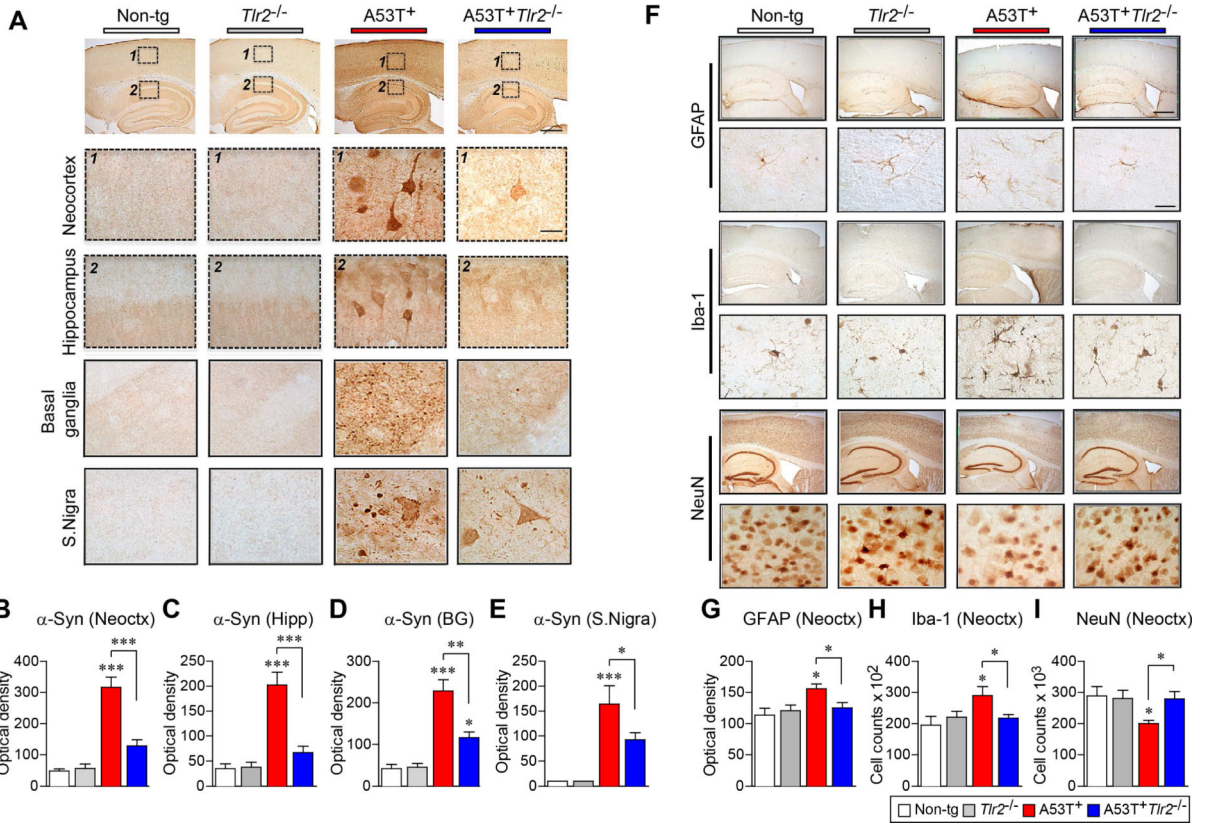


**Figure 2. α-synuclein Deposition, Neuroinflammation, and Neurodegeneration in Models of PD**

(A) Representative immunohistochemical staining of α-synuclein in the neocortex, hippocampus, basal ganglia, and substantia nigra of 5 month age-matched non-tg and tg mice brains. See Figure S2A for α-synuclein immunohistochemical analysis of 9 month age-matched group. Also see Figure S2D-S2H for human α-synuclein immunohistochemical analysis. Scale bars, 250 μm (low magnification) and 25 μm (high magnification).

(B-E) Optical density analysis of immunohistochemical immunoreactivity of α-synuclein in brain regions (n = 6 per each group; one-way ANOVA; \*p < 0.05, \*\*p < 0.01, \*\*\*p < 0.001). Data are represented as mean ± SEM.

(F) Representative immunohistochemical staining of GFAP, Iba-1, and NeuN in neocortex/hippocampus (low magnification) and neocortex (high magnification) of 5 month age-matched non-tg and tg mice brains. See Figures S2B and S2C for proinflammatory cytokine gene expression. Scale bars, 250 μm (low magnification) and 25 μm (high magnification).

(G-I) Optical density analysis of immunohistochemical immunoreactivity of GFAP, Iba-1, and NeuN in the neocortex regions (n = 6 per each group; one-way ANOVA; \*p < 0.05, \*\*p < 0.01). Data are represented as mean ± SEM.

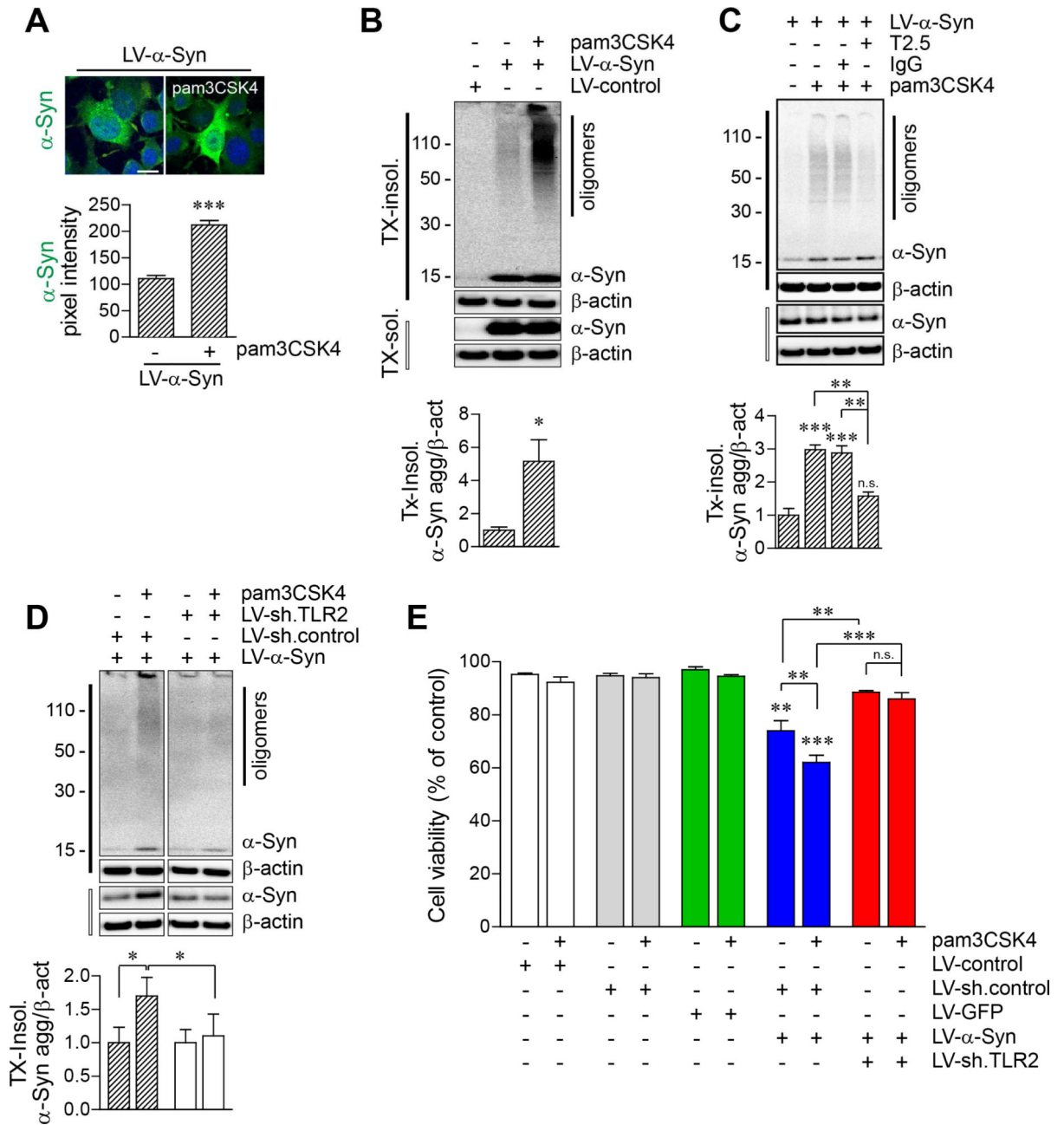


**Figure 3. Accumulation of Cytotoxic  $\alpha$ -synuclein Oligomers by TLR2 Activation in Neuronal Cells**

(A-C) dSY5Y cells were infected with either LV-control or LV- $\alpha$ -Syn, and treated with pam3CSK4 (10  $\mu$ g/ml) for 24 hours. See Figures S3A and S3B for TLR2 expression and activation in dSY5Y cells.

(A)  $\alpha$ -synuclein-expressing dSY5Y cells were immunolabeled with antibody against human  $\alpha$ -synuclein (syn211). Fluorescence intensity was analyzed in ten randomly chosen areas ( $n = 3$ ; unpaired  $t$ -test; \*\*\* $p < 0.001$ ). Data are represented as mean  $\pm$  SEM. Scale bar, 20  $\mu$ m.

(B) Western blot analysis for Tx-insoluble and Tx-soluble fractions. Tx-insoluble  $\alpha$ -synuclein oligomer levels were determined by densitometric quantification ( $n = 3$ ; unpaired  $t$ -test;  $*p < 0.05$ ). Data are represented as mean  $\pm$  SEM.

(C) Effect of TLR2 functional blocking antibody (T2.5) in accumulation of  $\alpha$ -synuclein oligomers by TLR2 agonist.  $\alpha$ -synuclein-expressing dSY5Y cells were treated with IgG (10  $\mu\text{g/ml}$ ) or T2.5 (10  $\mu\text{g/ml}$ ) for 30 minutes before addition of pam3CSK4 (10  $\mu\text{g/ml}$ ). Tx-insoluble  $\alpha$ -synuclein oligomer levels were determined by densitometric quantification ( $n = 3$ ; one-way ANOVA;  $**p < 0.01$ ,  $***p < 0.001$ ; n.s., not significant). Data are represented as mean  $\pm$  SEM.

(D) Effect of TLR2 knockdown in accumulation of  $\alpha$ -synuclein oligomers by TLR2 agonist. dSY5Y cell were infected with either combination of LV-sh.control/LV- $\alpha$ -Syn or LV- $\alpha$ -Syn/LV-sh.TLR2, and treated with pam3CSK4 (10  $\mu\text{g/ml}$ ) for 24 hours ( $n = 4$ ; unpaired  $t$ -test;  $*p < 0.05$ ). Data are represented as mean  $\pm$  SEM. See Figures S4A-S4C for construction and validation of LV-sh.TLR2.

(E) Cell viability analysis in dSY5Y cells. dSY5Y cells were infected with LV-control, LV-sh.control, LV-GFP, LV- $\alpha$ -Syn/LV-sh.control, or LV- $\alpha$ -Syn/LV-sh.TLR2, and treated with pam3CSK4 (10  $\mu\text{g/ml}$ ) for 24 hours ( $n = 4$ ; one-way ANOVA;  $*p < 0.05$ ,  $**p < 0.01$ ,  $***p < 0.001$ ; n.s., not significant). Data are represented as mean  $\pm$  SEM. See Figure S3C for cell viability analysis with TLR2 functional blocking antibody (T2.5).

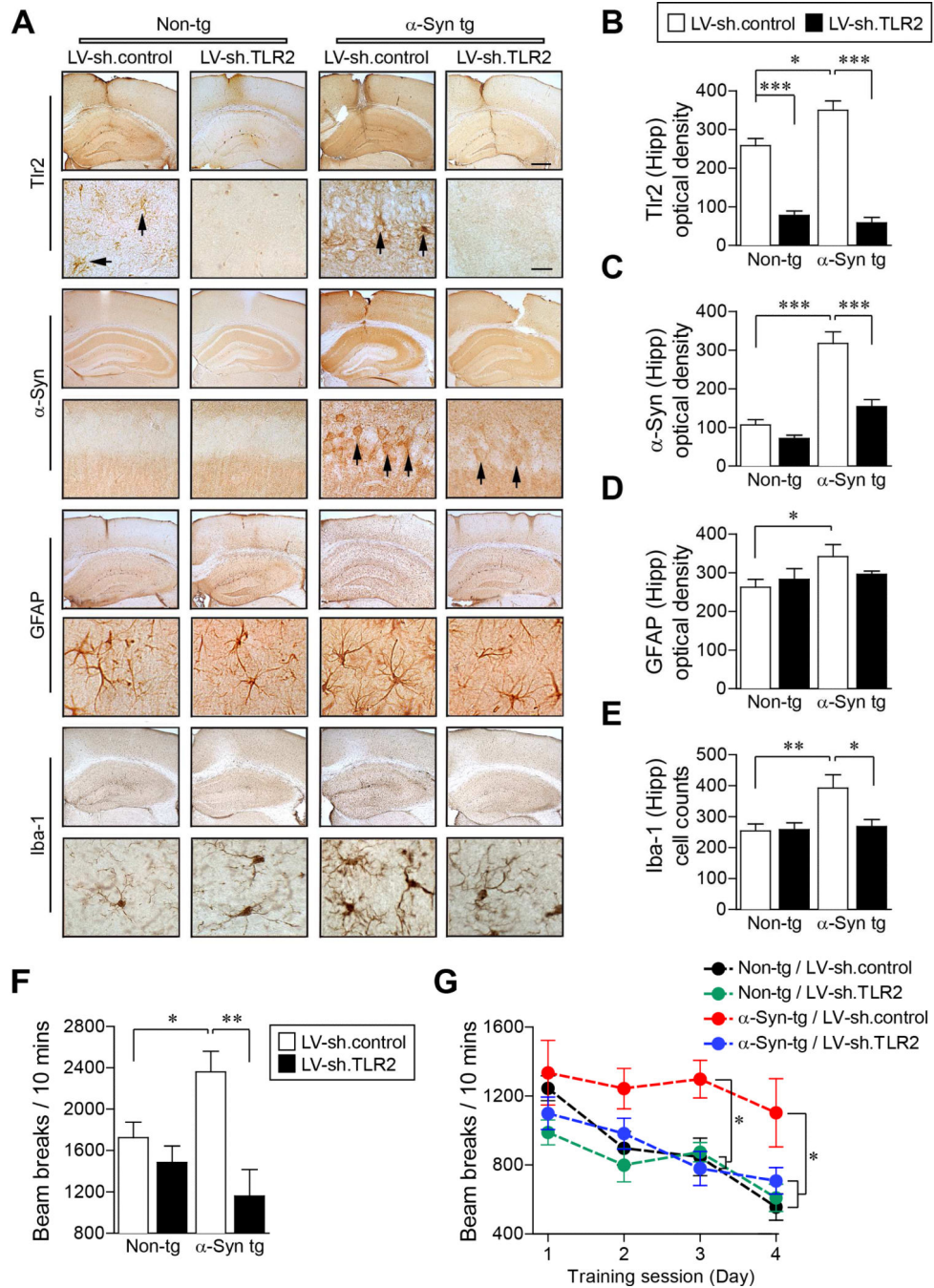


**Figure 4. Knockdown of Tlr2 Ameliorates α-synuclein Pathology and Behavioral Deficits in α-Syn tg Mice**

Either LV-sh.control or LV-sh.TLR2 was injected into hippocampus and striatum of non-tg and α-Syn tg (D line) mice.

(A) Representative immunohistochemical staining of Tlr2, α-synuclein, GFAP, and Iba-1 in neocortex/hippocampus (low magnification) and hippocampus (high magnification) of non-tg and α-Syn tg mice. See Figure S4D for α-synuclein/TLR2 double immune-labeling analysis. Scale bars, 250 μm (low magnification) and 25 μm (high magnification).

(B-E) Optical density analysis of immunohistochemical immunoreactivity of Tlr2,  $\alpha$ -synuclein, GFAP and Iba-1 in the hippocampus (n = 6 per group; one-way ANOVA; \*p < 0.05, \*\*p < 0.01, \*\*\*p < 0.001; n.s., not significant). Data are represented as mean  $\pm$  SEM. (F and G) Motor behavioral analysis of non-tg and  $\alpha$ -Syn tg mice using beam break test. Total beam breaks (F) and daily beam breaks (G) were recorded. (n = 5 per each group; one-way ANOVA; \*p < 0.05, \*\*p < 0.01). Data are represented as mean  $\pm$  SEM.

Author Manuscript

Author Manuscript

Author Manuscript

Author Manuscript

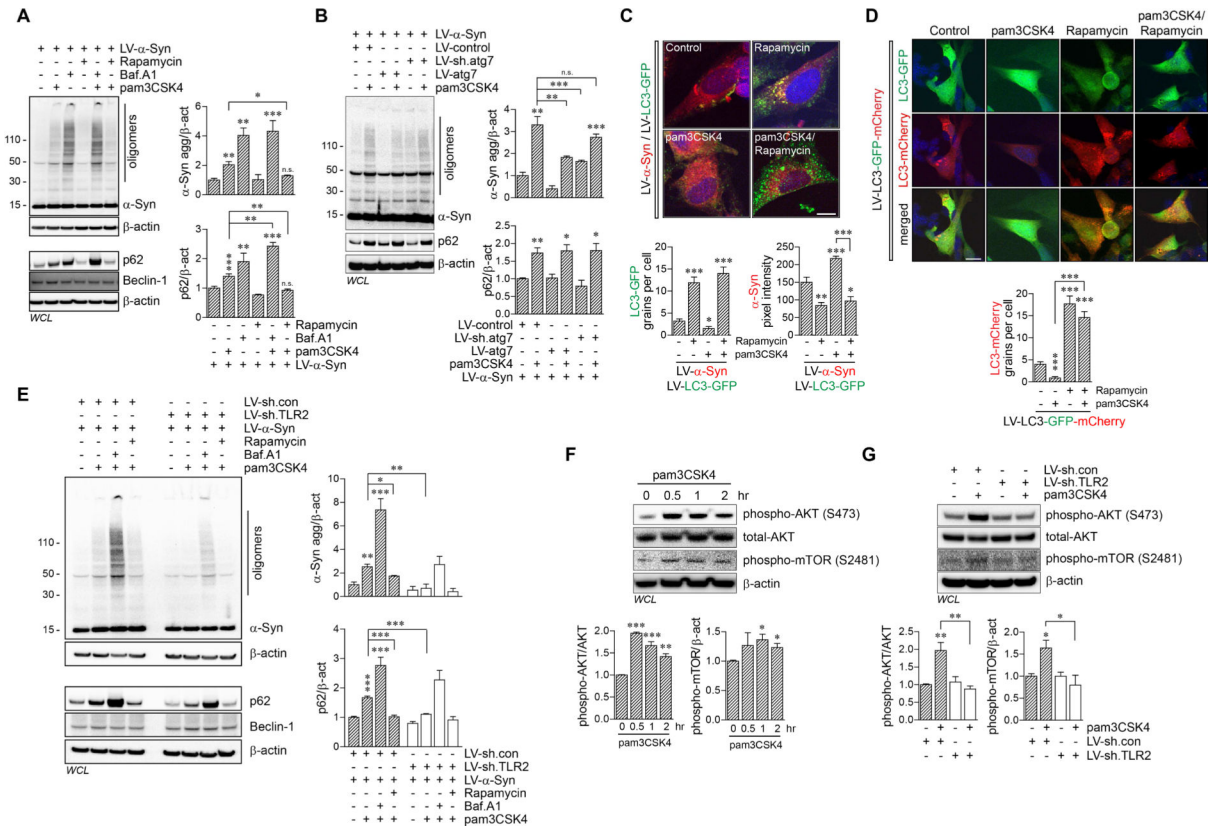


**Figure 5. Impairment of Autophagy by TLR2 Activation through AKT/mTOR Signaling Process, Results in Accumulation of  $\alpha$ -Synuclein Aggregates in Neuronal Cells**

(A) dSY5Y cells were infected with LV- $\alpha$ -Syn, and pre-treated with bafilomycin A1 (Baf.A1, 100 nM) for 30 min, prior to adding pam3CSK4 (10  $\mu$ g/ml) or simultaneously treated with pam3CSK4 and rapamycin (100  $\mu$ M). After 24 hours incubation, whole cell lysates were analyzed by western blot analysis. The levels of  $\alpha$ -synuclein oligomers and p62/SQSTM1 were determined by densitometric quantification ( $n = 3$ ; one-way ANOVA; \* $p < 0.05$ , \*\* $p < 0.01$ , \*\*\* $p < 0.001$ ; n.s., not significant). Data are represented as mean  $\pm$  SEM.

(B) dSY5Y cells were infected with indicated combination of lentiviral vectors, and treated pam3CSK4 (10  $\mu$ g/ml) for 24 hours. Whole cell lysates were analyzed by western blot analysis. The levels of  $\alpha$ -synuclein oligomers and p62/SQSTM1 were determined by densitometric quantification ( $n = 3$ ; one-way ANOVA; \* $p < 0.05$ , \*\* $p < 0.01$ , \*\*\* $p < 0.001$ ; n.s., not significant). Data are represented as mean  $\pm$  SEM.

(C and D) dSY5Y cells were infected with either LV- $\alpha$ -Syn/LV-LC3-GFP or LV-LC3-GFP-mCherry (pH-sensitive-GFP-mCherry tag), and treated with pam3CSK4 (10  $\mu$ g/ml) and/or rapamycin (100  $\mu$ M) for 24 hours. See also Figure S6 for autophagy analysis in non-tg and tg mice brains.

(C) Formations of LC3-GFP punctae (green) and immunoreactivity of  $\alpha$ -synuclein (red) were analyzed by confocal microscope. LC3-GFP grains and  $\alpha$ -synuclein fluorescence intensity were analyzed in ten randomly chosen areas from three independent experiments ( $n = 3$ ; one-way ANOVA; \* $p < 0.05$ , \*\* $p < 0.01$ , \*\*\* $p < 0.001$ ). Data are represented as mean

± SEM. Scale bar, 20 µm. See Figure S5A for LV-control/LV-LC3-GFP delivered control experiment.

(D) Formations of LC3-mCherry punctae (red) were analyzed by confocal microscope. The numbers of LC3-mCherry grains were analyzed in ten randomly chosen areas from three independent experiments (n = 3; one-way ANOVA; \*\*\*p < 0.001). Data are represented as mean ± SEM. Scale bar, 20 µm.

(E) dSY5Y cells were infected with either combination of LV-α-Syn/LV-sh.control or LV-α-Syn/LV-sh.TLR2, and pre-treated with bafilomycin A1 (100 nM) for 30 min, prior to adding pam3CSK4 (10 µg/ml) or simultaneously treated with pam3CSK4 and rapamycin (100 µM). After 24 hours incubation, whole cell lysates were analyzed by western blot analysis. The levels of α-synuclein oligomers and p62/SQSTM1 were determined by densitometric quantification (n = 3; one-way ANOVA; \*p < 0.05, \*\*p < 0.01, \*\*\*p < 0.001). Data are represented as mean ± SEM. See Figure S5B for time-course analysis of α-synuclein and p62/SQSTM1 accumulation by TLR2 activation. Also see Figures S5C and S5D for western blot analysis for ubiquitin, Lamp2a, and lysosomal α-synuclein.

(F) dSY5Y cells were treated with pam3CSK4 (10 µg/ml) for indicated hours, and whole cell lysates were analyzed by western blot analysis. The levels of phosphorylated AKT (S473) and phosphorylated mTOR (S2481) were determined by densitometric quantification (n = 3; one-way ANOVA; \*p < 0.05, \*\*p < 0.01, \*\*\*p < 0.001). Data are represented as mean ± SEM. (G) dSY5Y cells were infected with LV-sh.control or LV-sh.TLR2, and treated with pam3CSK4 (10 µg/ml) for 1 hour. Whole cell lysates were analyzed by western blot analysis. The levels of phosphorylated AKT (S473) and phosphorylated mTOR (S2481) were determined by densitometric quantification (n = 3; one-way ANOVA; \*p < 0.05, \*\*p < 0.01). Data are represented as mean ± SEM.

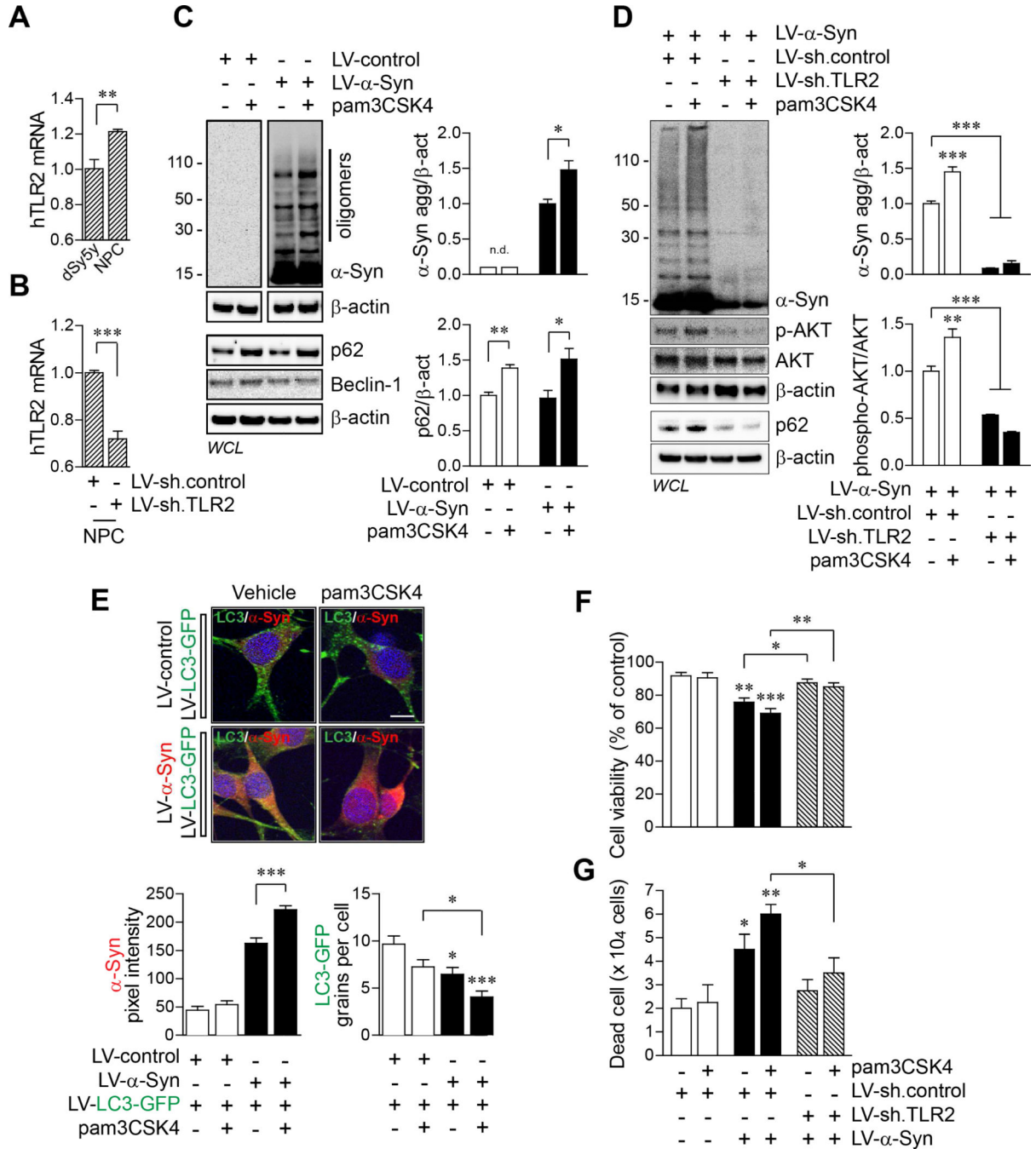


**Figure 6. Activation of TLR2 Inhibits Autophagy and Induces Accumulation of α-synuclein in Human Neural Precursor Cells**

(A) The human TLR2 mRNA levels from dSY5Y cells and human neural precursor cells (NPCs). (n = 4; unpaired *t*-test; \* \*\*p < 0.01). Data are represented as mean ± SEM.

(B) Knockdown of TLR2 in NPCs by LV-sh.TLR2 infection. (n = 4; unpaired *t*-test; \*\*\*p < 0.001). Data are represented as mean ± SEM.

(C) NPCs were infected with LV-control or LV-α-Syn, and treated with pam3CSK4 (10 μg/ml) for 24 hours. Whole cell lysates were analyzed by western blot analysis. The levels of α-synuclein oligomers and p62/SQSTM1 were determined by densitometric



quantification ( $n = 3$ ; unpaired  $t$ -test;  $*p < 0.05$ ,  $**p < 0.01$ ; n.d., not detected). Data are represented as mean  $\pm$  SEM.

(D) NPCs were infected with either combination of LV-sh.control/LV- $\alpha$ -Syn or LV-sh.TLR2/LV- $\alpha$ -Syn, and treated with pam3CSK4 (10  $\mu\text{g/ml}$ ) for 24 hours. Whole cell lysates were analyzed by western blot analysis. The levels of  $\alpha$ -synuclein oligomers and phosphorylated-AKT were determined by densitometric quantification ( $n = 3$ ; one-way ANOVA;  $*p < 0.05$ ,  $***p < 0.001$ ). Data are represented as mean  $\pm$  SEM.

(E) NPCs were infected with either combination of LV-control/LV-LC3-GFP or LV- $\alpha$ -Syn/LV-LC3-GFP, and treated with pam3CSK4 (10  $\mu\text{g/ml}$ ) for 24 hours. Formations of LC3-GFP punctae (green),  $\alpha$ -synuclein immunoreactivity (red, Syn211), and nuclei (DAPI, blue) were analyzed by confocal microscope. LC3-GFP grains and  $\alpha$ -synuclein fluorescence intensity were analyzed in ten randomly chosen areas ( $n = 3$ ; one-way ANOVA;  $*p < 0.05$ ,  $***p < 0.001$ ). Data are represented as mean  $\pm$  SEM. Scale bar, 20  $\mu\text{m}$ .

(F and G) Cytotoxicity analysis in NPCs. NPCs were infected with LV-sh.control, LV- $\alpha$ -Syn/LV-sh.control, or LV- $\alpha$ -Syn/LV-sh.TLR2, and treated with pam3CSK4 (10  $\mu\text{g/ml}$ ) for 24 hours. Cytotoxicity was determined by cell viability assay (F) and number of dead cells (G) ( $n = 4$ ; one-way ANOVA;  $*p < 0.05$ ,  $**p < 0.01$ ,  $***p < 0.001$ ). Data are represented as mean  $\pm$  SEM.

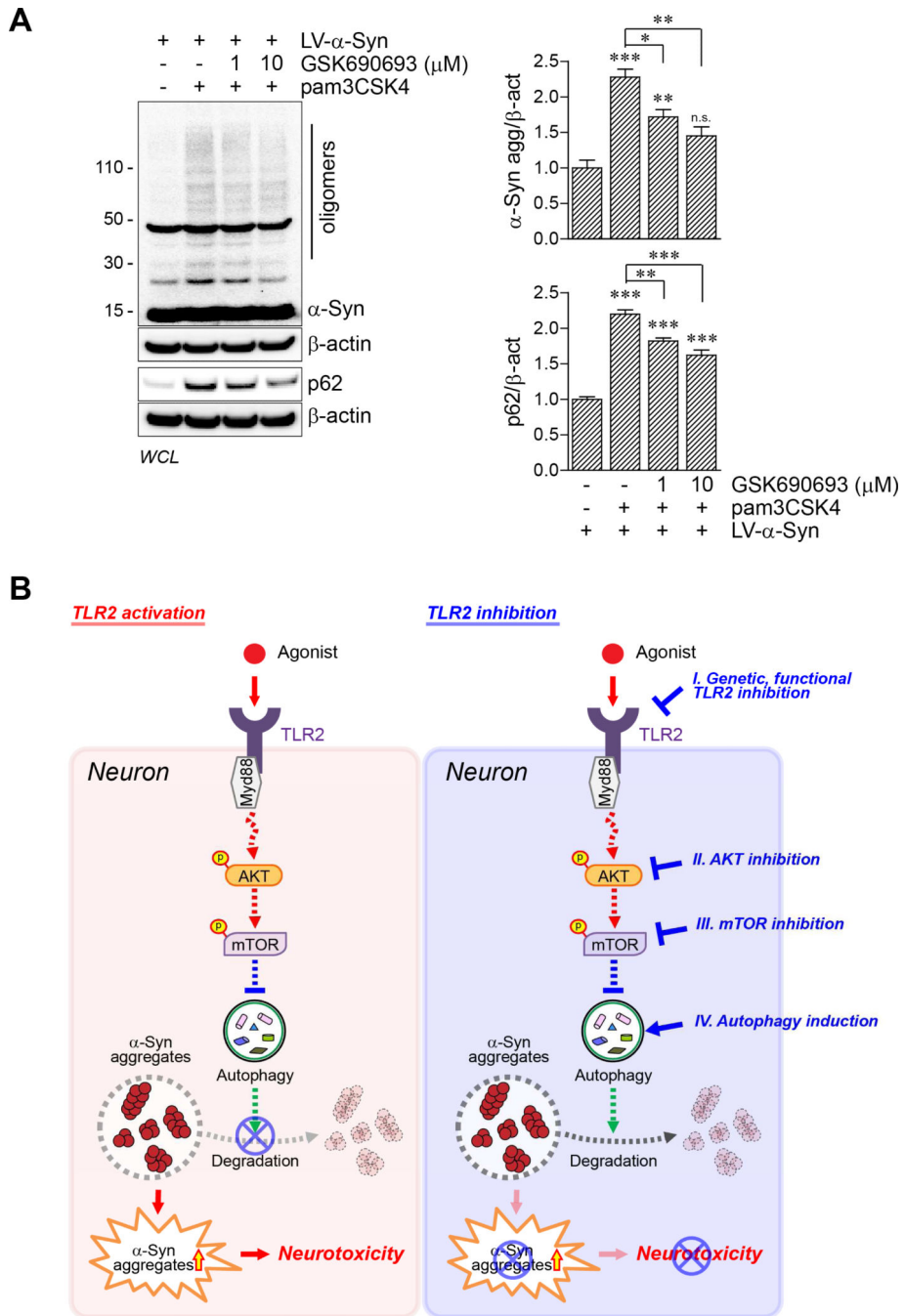


**Figure 7. Model for  $\alpha$ -synuclein accumulation by autophagy dysregulation via TLR2/AKT/mTOR signaling pathway in neuron**

(A) dSY5Y cells were infected with LV- $\alpha$ -Syn, and treated with pam3CSK4 (10  $\mu$ g/ml) or simultaneously treated with pam3CSK4 and GSK690693 (1 or 10  $\mu$ M) for 24 hours. Whole cell lysates were analyzed by western blot analysis. The levels of  $\alpha$ -synuclein oligomers and p62/SQSTM1 were determined by densitometric quantification (n = 3; one-way ANOVA; \*p < 0.05, \*\*p < 0.01, \*\*\*p < 0.001; n.s., not significant). Data are represented as mean  $\pm$  SEM.

(B) Activation of TLR2 induces activation of AKT/mTOR signaling thereby inhibiting autophagy in neurons resulting in accumulation of  $\alpha$ -synuclein oligomers and neurotoxicity. This model suggests that both regulation of  $\alpha$ -synuclein oligomerization and TLR2/downstream signaling are potential therapeutic targets for synucleinopathies, including PD and DLB. See also Figure S7.

Author Manuscript

Author Manuscript

Author Manuscript

Author Manuscript